Stress intensity factors of a central interface crack in a bonded finite plate and periodic interface cracks under arbitrary material combinations

Yu Zhang *, Nao-Aki Noda, Ken-Taro Takaishi, Xin Lan

Department of Mechanical Engineering, Kyushu Institute of Technology, 1-1 Sensui-cho, Tobata-ku, Kitakyushu-shi, Fukuoka 804-8550, Japan

ARTICLE INFO

ABSTRACT

Although a lot of interface crack problems were previously treated, few solutions are available under arbitrary material combinations. This paper deals with a central interface crack in a bonded finite plate and periodic interface cracks. Then, the effects of material combination and relative crack length on the stress intensity factors are discussed. A useful method to calculate the stress intensity factor of interface crack is presented with focusing on the stress at the crack tip calculated by the finite element method.

© 2011 Published by Elsevier Ltd.

1. Introduction

Although a lot of papers were published, several fundamental problems have not been solved yet for interface cracks. For stress intensity factors of the interface crack, the most fundamentally known is the results for the bonded infinite plate subjected to the internal stress σ (see Fig. 1a), which is expressed in the following equations.

$$K_I + iK_{II} = (F_I + iF_{II})(1 + 2i\varepsilon)\sigma\sqrt{\pi a}, \quad F_I = 1, \ F_{II} = 0 \tag{1}$$

$$\varepsilon = \frac{1}{2\pi}\ln\left[\left(\frac{\kappa_1}{G_1} + \frac{1}{G_2}\right) \middle/ \left(\frac{\kappa_2}{G_2} + \frac{1}{G_1}\right)\right] \tag{2}$$

$$k_m = \begin{cases} (3 - v_m)/(1 + v_m) & \text{(Plane stress)} \\ 3 - 4v_m & \text{(Plane strain)} \end{cases}$$

$$v_m : \text{(Poisson's ratio)} \quad (m = 1, \ 2)$$

$$G_m : \text{(Shear modulus)} \quad (m = 1, \ 2)$$

It should be noted that Fig. 1a is equivalent to Fig. 1b, and the stress intensity factors in Fig. 1c is different from the ones in Fig. 1a and b. In other words, an interface crack subjected to internal pressure in bonded infinite plate is equivalent to an interface crack subjected to $\sigma_y^\infty = \sigma$ and $\sigma_{x1}^\infty, \sigma_{x2}^\infty$ which produce $\varepsilon_{x1} = \varepsilon_{x2}$ on the interface [1,2]. Therefore, the stress intensity

---

* Corresponding author.
  E-mail address: zyzhangyu1225@yahoo.com (Y. Zhang).

Nomenclature

a, W	crack length and the plate width
r, θ	polar coordinates around the crack tip
G_1, G_2	shear modulus for material 1 and material 2
v_1, v_2	Poisson's ratio for material 1 and material 2
K_I, K_{II}	stress intensity factors
F_I, F_{II}	dimensionless stress intensity factors defined by $K_I + iK_{II} = (F_I + iF_{II})(1 + 2i\varepsilon)\sigma\sqrt{\pi a}$
$F_I^{(a)}, F_{II}^{(a)}$	dimensionless stress intensity factors for periodic interface cracks
$F_I^{(b)}, F_{II}^{(b)}$	dimensionless stress intensity factors for a central interface crack in bonded finite plate
σ_y^∞	tension stress applied at material 1 and material 2 in infinite y-direction
$\sigma_{x1}^\infty, \sigma_{x2}^\infty$	tension stress applied at material 1 and material 2 in infinite x-direction
$\varepsilon x_1, \varepsilon x_2$	strain in x-direction for material 1 and material 2
u_x	displacement in x-direction
σ_x, τ_{xy}	tension stress in x-direction and shear stress

$$\sigma_{x2}^\infty = \frac{1}{1+\kappa_2}\left[\frac{G_2}{G_1}(1+\kappa_1)\sigma_{x1}^\infty + \left\{3 - \kappa_2 - \frac{G_2}{G_1}(3-\kappa_1)\sigma_y^\infty\right\}\right]$$
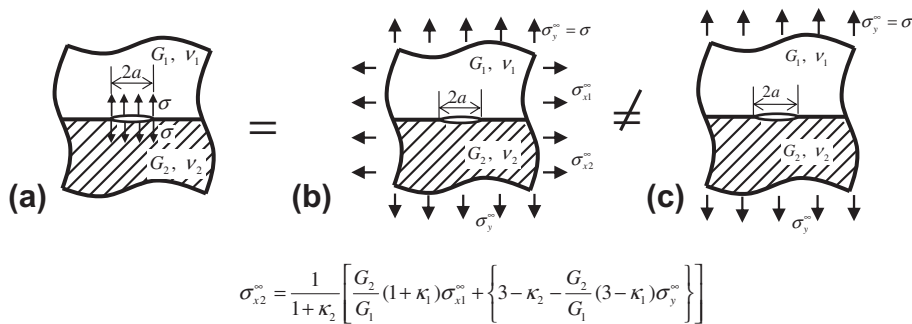
Fig. 1. Infinite plate subjected to (a) internal pressure, (b) σ_y^∞, σ_{x1}^∞, σ_{x2}^∞ and (c) σ_y^∞.

factors for Fig. 1a and b are expressed as the sum of the ones of Fig. 2a–c. Since the fundamental solutions for Fig. 2a–c were not available, the authors have shown the stress intensity factors for those problems under arbitrary material combination (see Fig. 3a and b) [2].

However, an interface crack in a bonded finite plate has not been discussed yet under arbitrary material combination. Although a lot of related studies were published previously, few solutions are available under arbitrary material combinations. In this paper, therefore, periodic interface cracks as shown in Fig. 4a will be treated in comparison with a central interface crack in bonded finite plates as shown in Fig. 4b. Then, the effects of relative of crack length on the stress intensity factors will be analyzed explicitly under arbitrary material combination. In Fig. 4a, along $x = (1 + 2n)W$ (n is the integer) the boundary conditions are $u_x = 0$, $\tau_{xy} = 0$ but $\sigma_x \neq 0$. On the other hand, in Fig. 4b along $x = \pm W$ the boundary conditions are $\sigma_x = 0$, $\tau_{xy} = 0$.

In this paper, a useful method to calculate the stress intensity factor of interface crack is presented with focusing on the stress at the crack tip calculated by the finite element method [3].

2. Analysis method

The analysis method used in this research is based on the stresses at the crack tip calculated by FEM. By using the proportional stress fields for the reference and given problems, stress intensity factors can be obtained with a good accuracy [4]. For example, for model I crack in homogenous plates, the stress distribution near the crack tip ($\theta = 0$) can be expressed by Eq. (3).

$$\sigma_y = K_I/\sqrt{2\pi r} \tag{3}$$

It is confirmed that the error of FEM mainly comes from the mesh around the crack tip. Therefore if the same mesh size and pattern are applied to the reference and given unknown problems, stress intensity factors K_I can be obtained from the stresses σ_y calculated by FEM. At a given distance r the following relationship can be obtained.

$$K_I/\sigma_y = const \tag{4}$$

If different crack problems A and B are analyzed by applying the same FEM mesh, the following equation can be given at the same distance from the crack tip.
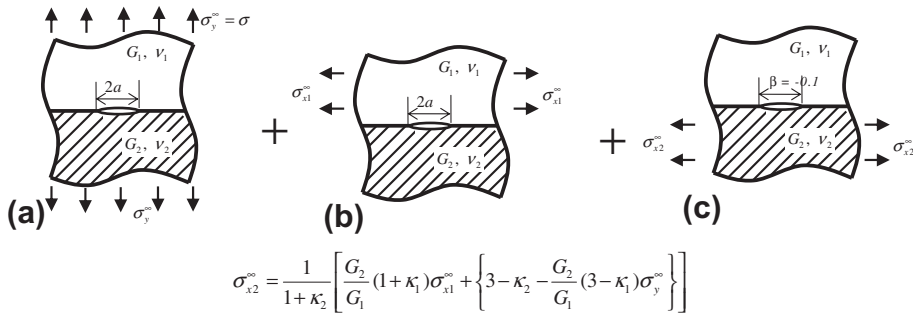
$$\sigma_{x2}^{\infty} = \frac{1}{1+\kappa_2}\left[\frac{G_2}{G_1}(1+\kappa_1)\sigma_{x1}^{\infty} + \left\{3-\kappa_2 - \frac{G_2}{G_1}(3-\kappa_1)\sigma_y^{\infty}\right\}\right]$$

Fig. 2. Infinite plate subjected to (a) σ_y^{∞}, (b) σ_{x1}^{∞} and (c) σ_{x2}^{∞}.
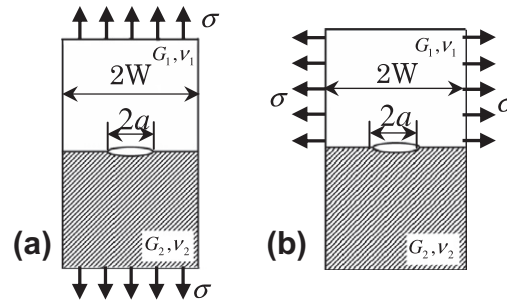

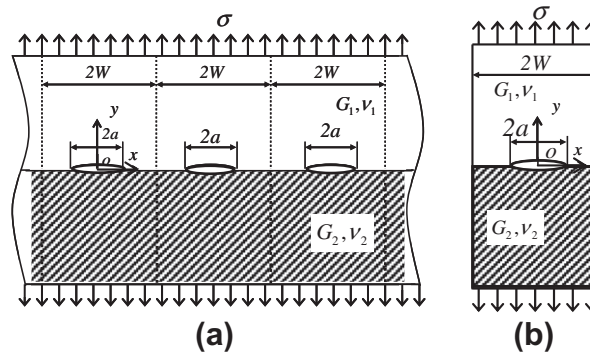**Fig. 3.** Bonded plate with a central interface crack with $a/W \to 0$.

Fig. 4. (a) Periodic interface cracks in an infinite bonded plate and (b) a central interface crack in a bonded plate.

$$\left[K_I^*/\sigma_y^*\right]_A = \left[K_I/\sigma_y\right]_B \tag{5}$$

Here, an asterisk ($*$) means the values of the reference problem. By using Eq. (5) with stress values at crack tip calculated by FEM, accurate stress intensity factors in homogenous plates were successfully obtained by Nisitani et al. [4,5].

Although this method cannot be applied to interface crack problems without difficulty, an effective method was recently proposed by Oda et al. [3] successfully to analyze interface crack problems. It is well known that there exists oscillation singularity at the interface crack tip. From the stresses σ_y, τ_{xy} along the interface crack tip, stress intensity factors are defined as shown in Eq. (6).

$$\sigma_y + i\tau_{xy} = \frac{K_I + iK_{II}}{\sqrt{2\pi r}}\left(\frac{r}{2a}\right)^{i\varepsilon}, \quad r \to 0, \tag{6}$$

From Eq. (6), it is known that because stress intensity factors for interface crack and the crack in homogenous material are different, it is difficult to separate modes absolutely. So it is necessary to obtain the following equation from Eq. (6)

$$K_I = \lim_{r \to 0} \sqrt{2\pi r}\sigma_y \left(\cos Q + \frac{\tau_{xy}}{\sigma_y} \sin Q \right), \tag{7}$$

$$K_{II} = \lim_{r \to 0} \sqrt{2\pi r}\tau_{xy} \left(\cos Q + \frac{\sigma_y}{\tau_{xy}} \sin Q \right), \tag{8}$$

$$Q = \varepsilon \ln \left(\frac{r}{2a} \right). \tag{9}$$

If the distance r is given as a constant, the following equation can be obtained.

$$Q^* = Q, \quad \frac{\tau_{xy}^*}{\sigma_y^*} = \frac{\tau_{xy}}{\sigma_y} \tag{10}$$

Therefore if Eq. (10) is satisfied, Eq. (11) may be derived from Eq. (7) and Eq. (8). In such case, oscillatory items of the reference and unknown problems are changed into the same.

$$\frac{K_I^*}{\sigma_y^*} = \frac{K_I}{\sigma_y}, \quad \frac{K_{II}^*}{\tau_{xy}^*} = \frac{K_{II}}{\tau_{xy}} \tag{11}$$

Here, $\sigma_{y0,FEM}^*$, $\tau_{xy0,FEM}^*$ are stresses of reference problem calculated by FEM, and $\sigma_{y0,FEM}$, $\tau_{xy0,FEM}$ are stresses of given unknown problem. Stress intensity factors of the given unknown problem can be obtained by:

$$K_I = \frac{\sigma_{y0,FEM}}{\sigma_{y0,FEM}^*} K_I^* \tag{12}$$

$$K_{II} = \frac{\tau_{y0,FEM}}{\tau_{y0,FEM}^*} K_{II}^* \tag{13}$$

Stress intensity factors of the reference problem are defined by Eq. (14).

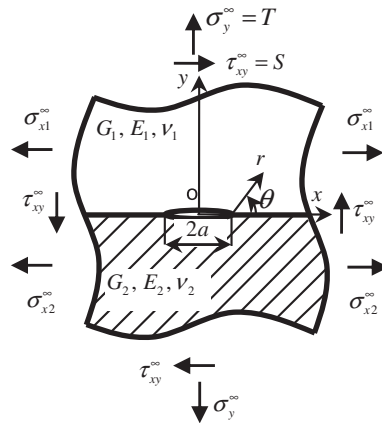$$K_I^* + iK_{II}^* = (T + iS)\sqrt{\pi a}(1 + 2i\varepsilon) \tag{14}$$

Fig. 5. Reference problem ($\varepsilon_{x1} = \varepsilon_{x2}$ at $y = 0$).

Table 1
Dimensionless stress intensity factors of crack in Fig. 3a with different a/W.

	a/W	$\alpha = 0.75$, $\beta = 0$	$\alpha = 0.75$, $\beta = 0$	$\alpha = 0.75$, $\beta = 0$
F_I	1/1620	0.93955	0.90859	0.95516
	1/3240	0.93955	0.90883	0.95515
	1/6480	0.93982	0.90943	0.95514
	→0	0.94002	0.91003	0.95513
F_{II}	1/1620	2.21×10^{-4}	2.59×10^{-4}	1.11×10^{-4}
	1/3240	1.10×10^{-4}	1.28×10^{-4}	5.53×10^{-5}
	1/6480	5.51×10^{-5}	6.42×10^{-5}	2.76×10^{-5}
	→0	0	0	0

Regarding the reference problem in Fig. 5, denote $\sigma_{y0,FEM}^{T=1,S=0*}$, $\tau_{xy0,FEM}^{T=1,S=0*}$ are values of stresses for $(T, S) = (1, 0)$ and $\sigma_{y0,FEM}^{T=0,S=1*}$, $\tau_{xy0,FEM}^{T=0,S=1*}$ are ones for $(T, S) = (0, 1)$. In order to satisfy Eq. (10), stresses at the crack tip of the reference problem are expressed as

$$\sigma_{y0,FEM}^* = \sigma_{y0,FEM}^{T=1,S=0*} \times T + \sigma_{y0,FEM}^{T=0,S=1*} \times S,$$
$$\tau_{xy0,FEM}^* = \tau_{xy0,FEM}^{T=1,S=0*} \times T + \tau_{xy0,FEM}^{T=0,S=1*} \times S,$$

(15)

By substituting Eq. (10) into Eq. (15) with $T = 1$, the value of S is obtained as

$$S = \frac{\sigma_{y0,FEM} \times \tau_{xy0,FEM}^{T=1,S=0*} - \tau_{xy0,FEM} \times \sigma_{y0,FEM}^{T=1,S=0*}}{\tau_{xy0,FEM} \times \sigma_{y0,FEM}^{T=0,S=1*} - \sigma_{y0,FEM} \times \tau_{xy0,FEM}^{T=0,S=1*}}$$

(16)

The problem that is subjected to $T = 1$ and S expressed by Eq. (16) is considered as the reference problem. Because the exact solution is known, the error of unknown problem can be evaluated by using the same mesh. In the following of the paper, results are shown using dimensionless stress intensity factors F_I, F_{II} defined in Eq. (1). Dundurs' bi-material parameters α, β are defined in Eq. (17).

$$\alpha = \frac{G_1(\kappa_2 + 1) - G_2(\kappa_1 + 1)}{G_1(\kappa_2 + 1) + G_2(\kappa_1 + 1)}, \beta = \frac{G_1(\kappa_2 - 1) - G_2(\kappa_1 - 1)}{G_1(\kappa_2 + 1) + G_2(\kappa_1 + 1)}$$
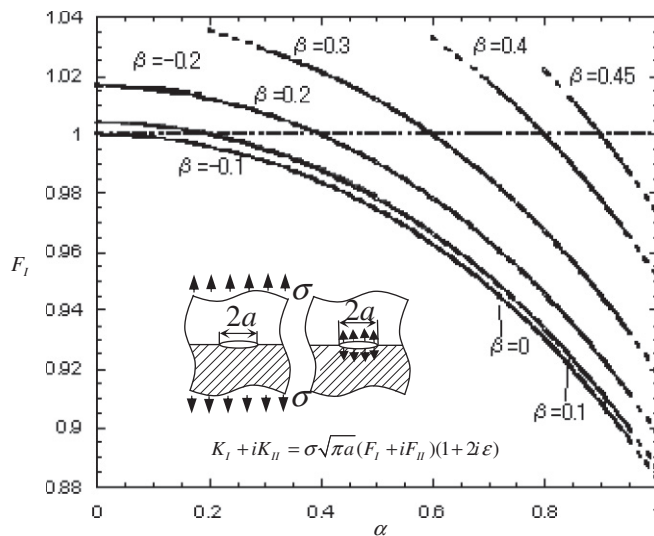
(17)

Fig. 6. F_1 of a central interface crack in a bonded infinite plate under uni-axal tension which is corresponding to Fig. 3a with $a/W \to 0$.
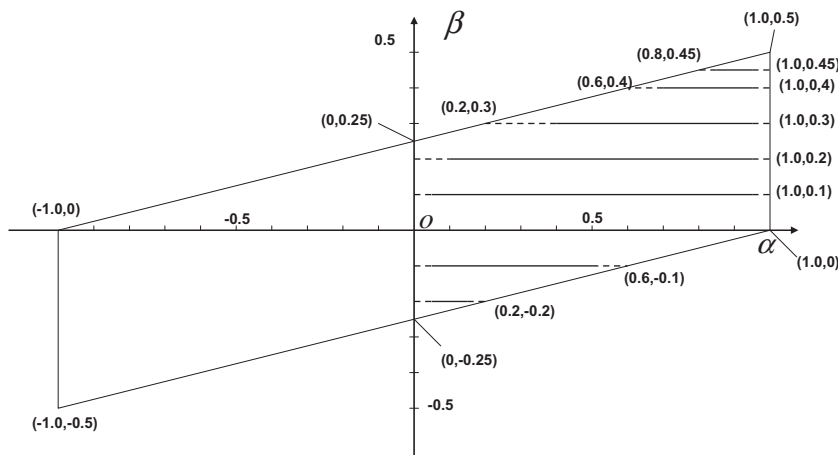

Fig. 7. The map of α and β.

3. Stress intensity factors for a central interface crack in a bonded infinite plate

In this paper, the solutions of infinite periodic cracks (see Fig. 4a) and a central interface crack in a bonded finite plate (see Fig. 4b) will be discussed. It should be noted that the limiting case $a/W \to 0$ in Fig. 4a coincides with the solution in Fig. 1a. On

Table 2
Dimensionless stress intensity factor F_I in Fig. 3a with $a/W \to 0$, $F_I = 1.0$ are marked by underlines.

α	β							
	−0.2	−0.1	0	0.1	0.2	0.3	0.4	0.45
0.00	1.017	1.004	_1.000_	1.004	1.017			
0.05	1.016	1.004	1.000	1.004	1.016	–	–	–
0.10	1.016	1.003	0.999	1.003	1.015	–	–	–
0.15	1.015	1.002	0.998	1.002	1.014	–	–	–
0.20	(1.013)	_1.000_	0.996	_1.000_	1.012	(1.036)	–	–
0.30	–	0.995	0.991	0.995	1.007	1.029	–	–
0.40	–	0.988	0.984	0.988	_1.000_	1.022	–	–
0.50	–	0.979	0.975	0.978	0.990	1.012	–	–
0.60	–	(0.966)	0.963	0.966	0.979	_1.000_	(1.033)	–
0.70	–	–	0.948	0.952	0.964	0.985	1.018	–
0.75	–	–	0.940	0.943	0.955	0.977	1.010	–
0.80	–	–	0.930	0.934	0.946	0.967	_1.000_	(1.022)
0.85	–	–	0.920	0.924	0.935	0.957	0.990	1.011
0.90	–	–	0.910	0.912	0.924	0.945	0.978	_1.000_
0.95	–	–	0.896	0.900	0.912	0.933	0.965	0.987
1.00	–	–	(0.882)	(0.886)	(0.898)	(0.919)	(0.952)	(0.974)

Table 3
Dimensionless stress intensity factors of crack in Fig. 3b with different a/W.

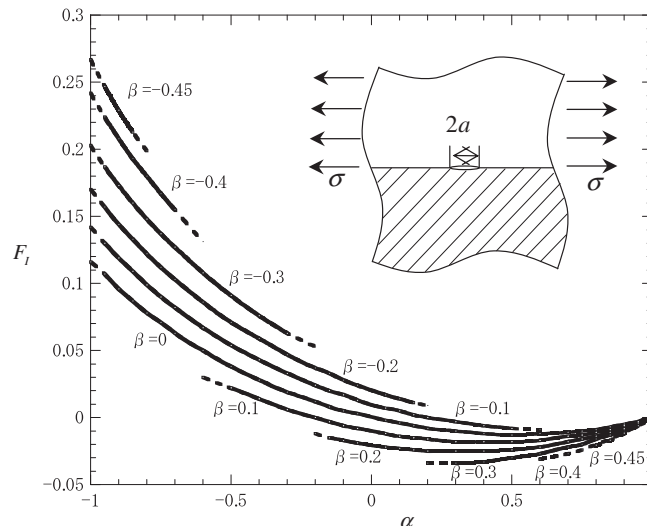|	a/W	$\alpha = 0.3, \beta = 0.2$	$\alpha = -0.75, \beta = 0$	$\alpha = -0.8, \beta = -0.4$
F_I	1/1620	−0.02540	0.07051	0.17962
	1/3240	−0.02539	0.07056	0.17960
	1/6480	−0.02539	0.07055	0.17959
	→0	−0.02539	0.07054	0.17958
F_{II}	1/1620	1.11×10^{-4}	2.59×10^{-4}	3.28×10^{-4}
	1/3240	5.53×10^{-4}	1.29×10^{-4}	1.64×10^{-4}
	1/6480	2.77×10^{-5}	6.46×10^{-5}	8.19×10^{-5}
	→0	0	0	0

Fig. 8. F_I of a central interface crack in a bonded infinite plate under $\sigma_{x1}^{\infty} = \sigma$ (see Fig. 3b with $a/W \to 0$).

the other hand, the limiting case $a/W \to 0$ in Fig. 4b coincides with the solution in Fig. 1c. Since the solution in Fig. 1a is expressed as Eq. (1), another fundamental solution of a central interface crack in bonded plate when $a/W \to 0$ will be indicated in the following [2].
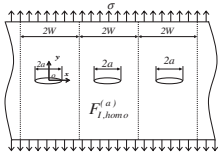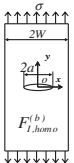
3.1. Effect of plate dimensions on the stress intensity factors

In order to discuss bonded infinite plates, it is necessary to consider the effect of the plate dimensions on the stress intensity factors because the finite element method cannot treat the infinite plates directly. The results of central interface crack

Table 4
Dimensionless stress intensity factor F_I in Fig. 3b with $a/W \to 0$.

α	β										
	−0.45	−0.4	−0.3	−0.2	−0.1	0	0.1	0.2	0.3	0.4	0.45
−1.00	(0.267)	(0.242)	(0.203)	(0.170)	(0.142)	(0.116)	–	–	–	–	–
−0.95	0.247	0.224	0.187	0.157	0.130	0.107	–	–	–	–	–
−0.90	0.229	0.208	0.173	0.144	0.119	0.096	–	–	–	–	–
−0.85	0.213	0.193	0.160	0.133	0.109	0.087	–	–	–	–	–
−0.80	(0.199)	0.180	0.148	0.122	0.099	0.078	–	–	–	–	–
−0.75	–	0.167	0.137	0.112	0.090	0.071	–	–	–	–	–
−0.70	–	0.155	0.127	0.103	0.082	0.063	–	–	–	–	–
−0.60	–	(0.131)	0.108	0.086	0.067	0.050	(0.030)	–	–	–	–
−0.50	–	–	0.091	0.071	0.054	0.038	0.022	–	–	–	–
−0.40	–	–	0.076	0.059	0.043	0.028	0.014	–	–	–	–
−0.30	–	–	0.063	0.047	0.033	0.019	0.006	–	–	–	–
−0.20	–	–	(0.053)	0.037	0.024	0.012	0.000	(−0.012)	–	–	–
−0.15	–	–	–	0.033	0.020	0.008	−0.003	−0.015	–	–	–
−0.10	–	–	–	0.028	0.017	0.005	−0.006	−0.017	–	–	–
−0.05	–	–	–	0.024	0.013	0.003	−0.008	−0.019	–	–	–
0.05	–	–	–	0.017	0.007	−0.002	−0.012	−0.022	–	–	–
0.10	–	–	–	0.014	0.005	−0.004	−0.014	−0.023	–	–	–
0.15	–	–	–	0.011	0.002	−0.006	−0.015	−0.024	–	–	–
0.20	–	–	–	(0.009)	0.000	−0.008	−0.016	−0.025	(−0.034)	–	–
0.30	–	–	–	–	−0.003	−0.010	−0.018	−0.025	−0.034	–	–
0.40	–	–	–	–	−0.006	−0.012	−0.018	−0.025	−0.033	–	–
0.50	–	–	–	–	−0.008	−0.013	−0.018	−0.024	−0.030	–	–
0.60	–	–	–	–	(−0.009)	−0.012	−0.017	−0.022	−0.027	(−0.031)	–
0.70	–	–	–	–	–	−0.011	−0.014	−0.018	−0.022	−0.027	–
0.75	–	–	–	–	–	−0.010	−0.013	−0.016	−0.020	−0.024	–
0.80	–	–	–	–	–	−0.009	−0.011	−0.014	−0.016	−0.020	(−0.021)
0.85	–	–	–	–	–	−0.007	−0.009	−0.011	−0.013	−0.016	−0.017
0.90	–	–	–	–	–	−0.005	−0.006	−0.008	−0.009	−0.011	−0.012
0.95	–	–	–	–	–	−0.003	−0.003	−0.004	−0.004	−0.006	−0.006
1.00	–	–	–	–	–	(−0.002)	(0.001)	(0.001)	(0.001)	(−0.001)	(0.001)

Table 5
The results of homogeneous plates.

a/W				

	Present analysis	Eq. (19)	Isida (9)	Eq. (20)
→0	1.0000	1.0000	1.0000	1.000
0.1	1.0042	1.0042	1.0060	1.006
0.2	1.0170	1.0170	1.0246	1.025
0.3	1.0399	1.0400	1.0577	1.058
0.4	1.0754	1.0753	1.1094	1.109
0.5	1.1282	1.1284	1.1867	1.186
0.6	1.208	1.2085	1.3033	1.303
0.7	1.335	1.3360	1.4882	1.487
0.8	1.561	1.5650	1.8160	1.814
0.9	2.105	2.1133	2.5776	2.577

in Fig. 3a are therefore investigated in Table 1 with varying $a/W = 1/1620,\ 1/3240,\ 1/6480$ and $\alpha = 0.75,\ \beta = 0,\ \alpha = 0.9,\ \beta = 0,\ \alpha = 0.75,\ \beta = 0.2$. It is seen that results of $a/W < 1/1620$ coincide each other and may have more than 3 digit accuracy. In other words, Table 1 shows that the results for $a/W = 1/1620$ can be used as the infinite plate $a/W \to 0$ with less than 0.09% error. It is also seen that $F_{II} \to 0$ as $a/W \to 0$ under arbitrary material combination. In the following sections, the results for the bonded infinite plate obtained as shown in Table 1 will be discussed.

3.2. Central interface crack in a bonded infinite plate under uni-axial tension

Fig. 6 shows the results of a central interface crack in a bonded infinite plate under uni-axial tension in the *y*-direction as shown in Fig. 3a. In Fig. 6, Dundur's parameter β is fixed, and the variations of F_I are depicted with varying parameter α. From Eq. (17), it is known that when material 1 and material 2 are exchanged, Dundur's parameters (α, β) become $(-\alpha, -\beta)$. Then the stress intensity factors (F_I, F_{II}) become $(F_I, -F_{II})$. Therefore all material combinations are considered in the range $\alpha > 0$ in Fig. 7.
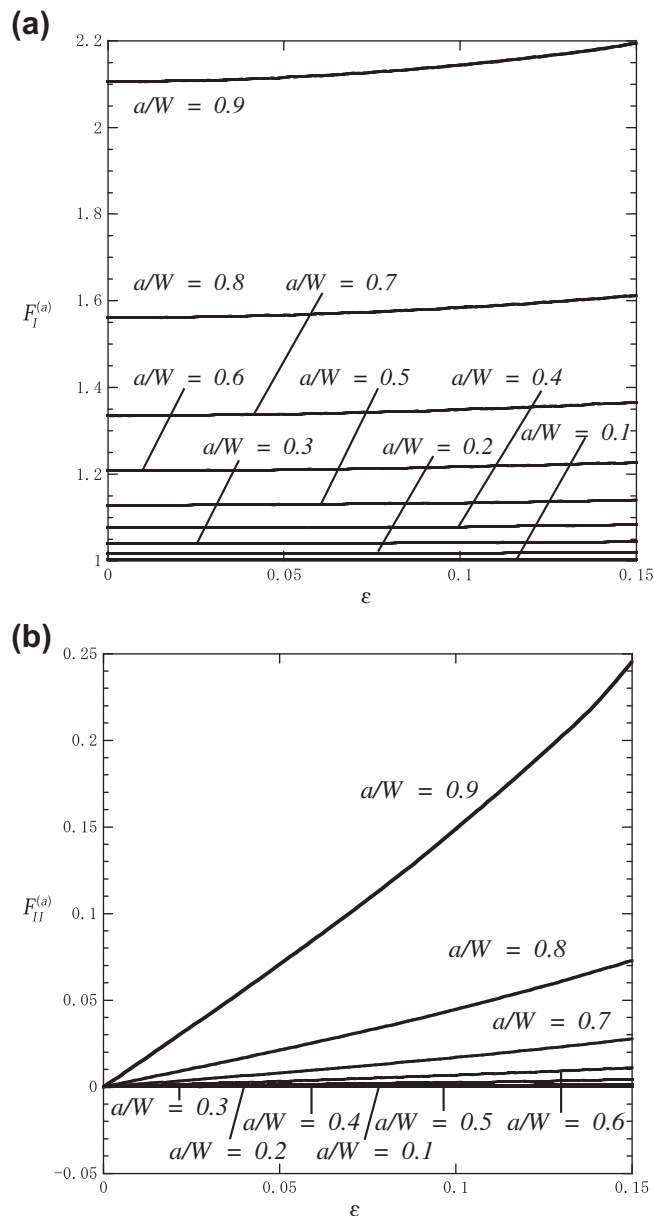

Fig. 9. The relationship between (a) $F_I^{(a)}$ vs. ε (b) $F_{II}^{(a)}$ vs. ε with different a/W in Fig. 4a.

In Fig. 6, the solid curves show the results of a central interface crack under remote tension $\sigma_y = \sigma$. The dashed lines are extended from solid lines because some cases of material combination are difficult to be obtained by the FEM. The dash-dotted line shows the results of that under internal pressure σ whose solution is known as $F_I = 1$ and $F_{II} = 0$. Fig. 6 shows the variation of $F_I = 0.882$–1.036, which has the minimum value $F_I = 0.882$ when $\alpha = 1.0$, $\beta = 0$, and the maximum value $F_I = 1.036$ when $\alpha = 0.2$, $\beta = 0.3$. It is also found that $F_{II} = 0$ for the full range of α, β. Therefore it may be concluded that central interface crack in a bonded infinite plate under remote tension of $\sigma = 1$ is equivalent to that under internal pressure of $\sigma = 0.882$–1.036. All the values in Fig. 6 are given in Table 2 with 3 decimal. From Fig. 6 and Table 3, we can conclude that $F_I > 1.0$ when $(\alpha + 2\beta)(\alpha - 2\beta) < 0$, $F_I = 1.0$ when $(\alpha + 2\beta)(\alpha - 2\beta) = 0$ and $F_I < 1$ when $(\alpha + 2\beta)(\alpha - 2\beta) > 0$. In Table 3, values for $F_I = 1.0$ are marked by underlines.

3.3. Central interface crack in a bonded infinite plate with material 1 under tension in the x-direction

Table 3 shows stress intensity factors of central interface crack shown in Fig. 3b with different relative crack size $a/W = 1/1620$, $1/3240$, $1/6480$ under different material combinations $\alpha = 0.3$, $\beta = 0.2$, $\alpha = -0.75$, $\beta = 0$, $\alpha = -0.8$, $\beta = -0.4$. It is seen that all the results coincide each other more than 3 digit when $a/W < 1/1620$.

Fig. 8 shows the results of bonded infinite plate $a/W \to 0$ with material 1 under tension in the x-direction. The dashed lines are extended from solid lines because some cases of material combination are difficult to be obtained by the FEM. In Fig. 8, β in each curve is fixed, and the variations of F_I are depicted with varying parameter α. Previously, it has been thought that tension in the x-direction does not contribute to the stress intensity factors [1]. However, as can be seen from Fig. 8, F_I is not 0 in current research. It should be noted that the stress intensity factor F_I is not zero under x-directional tension, except the case when $\varepsilon_{x1} = \varepsilon_{x2}$ is produced along the interface, and it has the minimum value $F_I = -0.034$ when $\alpha = 0.2$, $\beta = 0.3$, and the maximum value $F_I = 0.267$ when $\alpha = -1.0$, $\beta = -0.45$. It is also found that $F_{II} = 0$ for the central interface crack under x-directional tension. Therefore, it may be concluded that central interface crack in a bonded infinite plate with material 1 under x-directional remote tension is equivalent to that of under internal pressure of $\sigma = -0.034$ to 0.267. All the values in Fig. 8 are provided in Table 4.

4. Stress intensity factors for periodic interface cracks

Periodic interface cracks are one of the most fundamental problems. However, so far as the authors known, the solution is not available under arbitrary material combinations. Similarly to the problem of bonded infinite plate subjected to the internal pressure, the stress intensity factors only depend on the parameter ε. There, the parameters ε and β have the following relation. That is to say, stress intensity factors for periodic interface cracks only depend on ε or β.

$$\varepsilon = \frac{1}{2\pi} \ln\left(\frac{1-\beta}{1+\beta}\right) \tag{18}$$

First, the problem for homogenous material when $G_1 = G_2$ and $v_1 = v_2$ is treated. Exact solutions of stress intensity factors for Fig. 4a are expressed in the following [6–8].
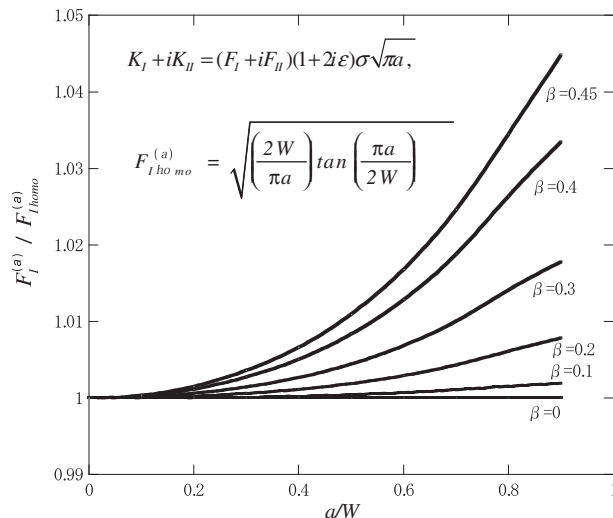

$$K_I + iK_{II} = (F_I + iF_{II})(1 + 2i\varepsilon)\sigma\sqrt{\pi a},$$

$$F_{I\,homo}^{(a)} = \sqrt{\left(\frac{2W}{\pi a}\right)\tan\left(\frac{\pi a}{2W}\right)}$$

Fig. 10. The relationship between $F_I^{(a)}/F_{Ihomo}^{(a)}$ vs. a/W in Fig. 4a.

$$F_{Ihomo}^{(a)} = \sqrt{\left(\frac{2W}{\pi a}\right)tan\left(\frac{\pi a}{2W}\right)} \tag{19}$$

Table 5 shows the results of periodic interface cracks $F_I^{(a)}$ for homogenous material. Comparing the present results with the exact solution in Eq. (19), it is found that they are coincide within the error 0.4%. Table 5 also shows the results of a central crack obtained by Isida [9] and the approximate solutions expressed in formula (20) [10].

$$F_{I\,homo}^{(b)} = \left\{1 - 0.025\left(\frac{a}{W}\right)^2 + 0.06\left(\frac{a}{W}\right)^4\right\}\sqrt{sec\left(\frac{\pi a}{2W}\right)} \tag{20}$$

Comparing the formulas of (19) and (20), it is seen that $F_I^{(b)}$ in Fig. 4b is about 20% larger than $F_I^{(a)}$ in Fig. 4a when the relative crack length is large.
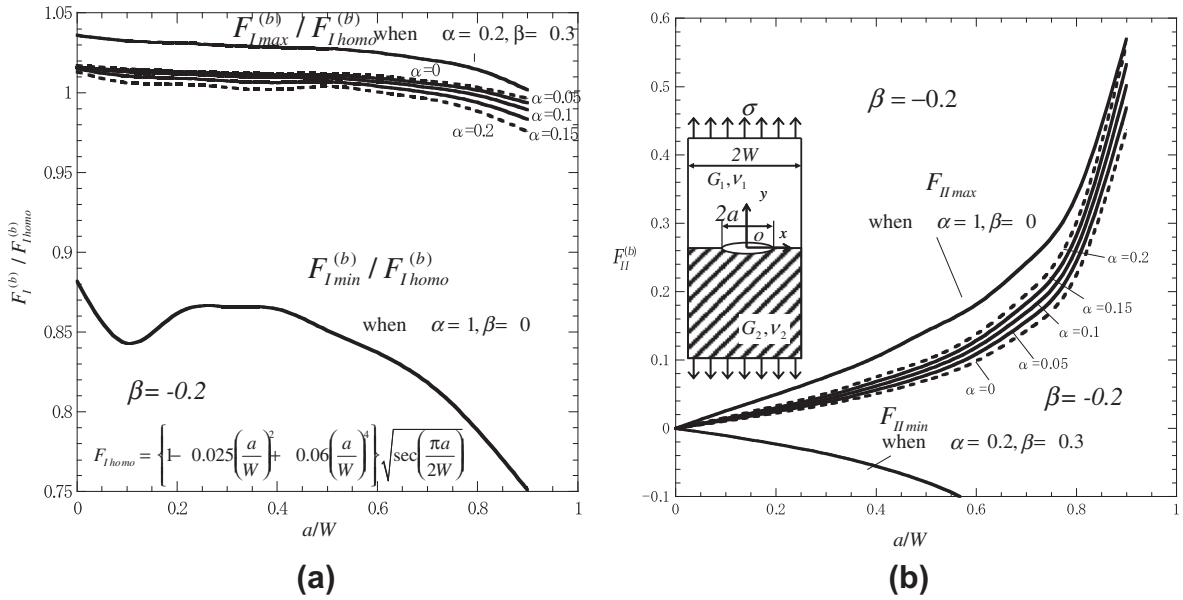
Fig. 11. (a) $F_I^{(b)}/F_{Ihomo}^{(b)}$ vs. a/W and (b) $F_{II}^{(b)}$ vs. a/W when $\beta = -0.2$.
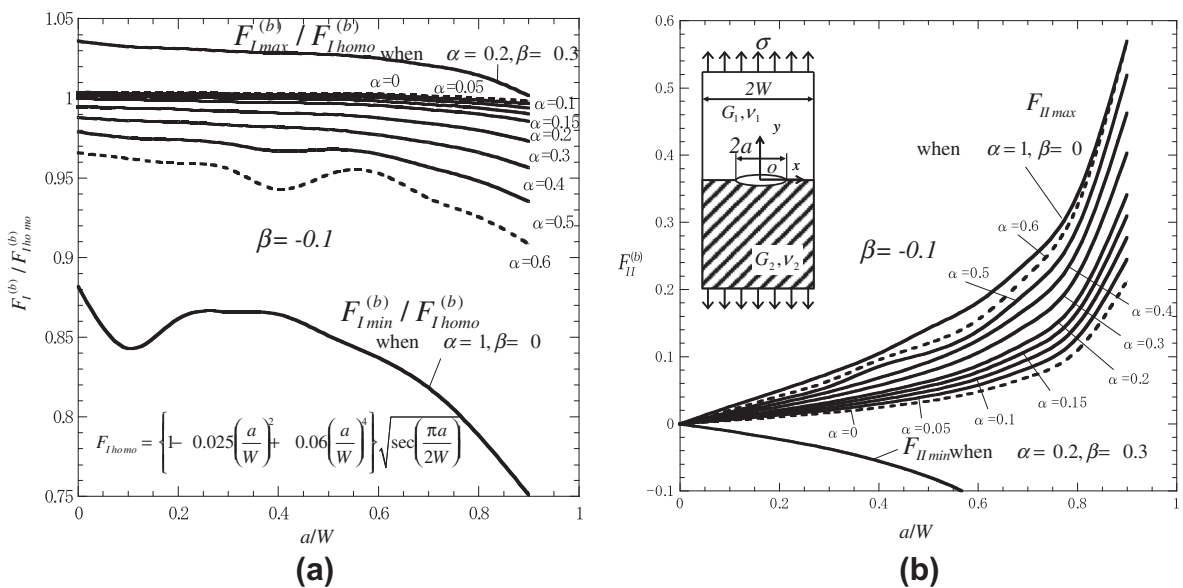
Fig. 12. (a) $F_I^{(b)}/F_{Ihomo}^{(b)}$ vs. a/W and (b) $F_{II}^{(b)}$ vs. a/W when $\beta = -0.1$.

Fig. 9a shows the relation between $F_I^{(a)}$ and ε with different a/W. From the figure, it is known that $F_I^{(a)}$ slightly increases with increasing ε when a/W is fixed, the increment is also larger when a/W is larger. Fig. 9b shows the relation between $F_{II}^{(a)}$ and ε with different a/W. Similarly to $F_I^{(a)}$, the values of $F_{II}^{(a)}$ also increases with increasing ε when a/W is fixed, and the increment becomes larger when a/W is larger.

Because parameters ε and β have the relationship in Eq. (18), the relation F_I and β also can be obtained. Fig. 10 shows the relation between F_I divided by $F_{I,homo}$ and β. From Fig. 10, it is known that $F_I/F_{I,homo}$ is nearly about 1 when a/W is small, and $F_I/F_{I,homo}$ becomes larger when a/W is larger.

5. Stress intensity factors for the interface crack in a bonded finite plate

Regarding another fundamental problem in Fig. 4b, effects of relative crack length a/W on stress intensity factors will be discussed under arbitrary combinations. When material 1 and material 2 are exchanged, Dundur's parameters (α, β) become
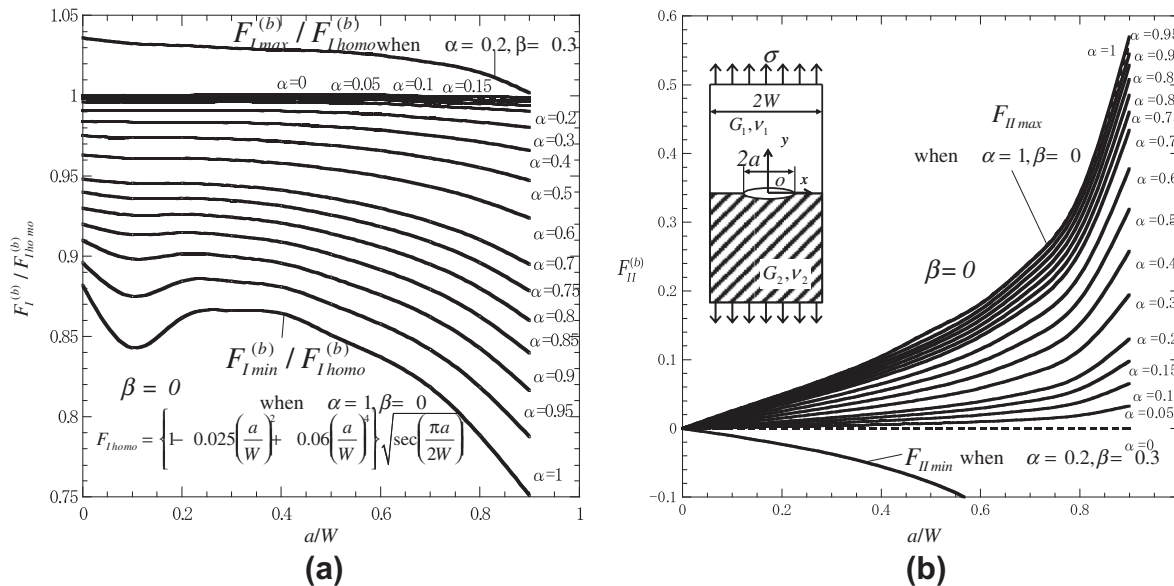

Fig. 13. (a) $F_I^{(b)}/F_{Ihomo}^{(b)}$ vs. a/W and (b) $F_{II}^{(b)}$ vs. a/W when β = 0.
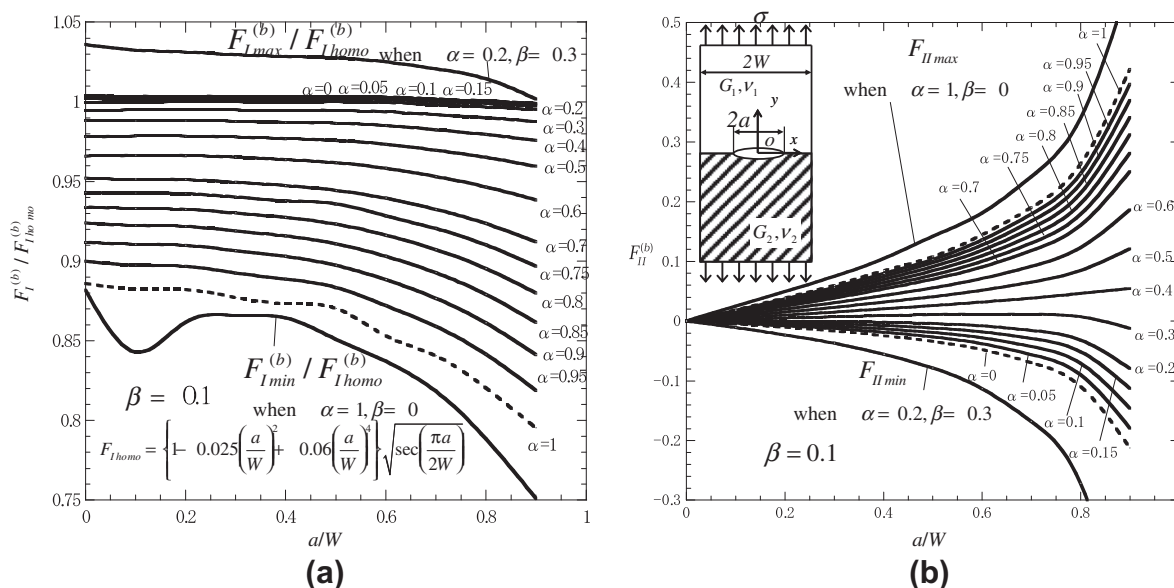

Fig. 14. (a) $F_I^{(b)}/F_{Ihomo}^{(b)}$ vs. a/W and (b) $F_{II}^{(b)}$ vs. a/W when β = 0.1.

$(-\alpha, -\beta)$; then the stress intensity factors (F_I, F_{II}) become $(F_I, -F_{II})$. Therefore all material combinations are considered in the range $\alpha > 0$ as shown in Fig. 7. For special material combinations indicated by the dashed lines in Fig. 7, calculations can not be executed by the current finite element method code, and the results for the region are obtained by extrapolation using the results that can be calculated.

The interface stress intensity factor $F_I^{(b)}$ is close to the solution $F_{I\ homo}$ of Isida [9] for homogenous materials as shown in Table 5. To discuss the variation $F_I^{(b)}$ clearly under different material combinations, the ration $F_I^{(b)}/F_{I\ homo}^{(b)}$ is indicated in Figs. 11a–18a. Those figures also show the maximum value $F_{Imax}^{(b)}$ and minimum value $F_{Imin}^{(b)}$ for all material combinations when β is fixed. Here, $F_{II}^{(b)}$ is directly shown from Figs. 11b to 18b with the maximum value $F_{IImax}^{(b)}$ and minimum value $F_{IImin}^{(b)}$ for all regions of material combination when β is fixed. When $a/W \rightarrow 0$, $F_{II}^{(b)}$ goes to 0, and the absolute value of $F_{II}^{(b)}$ monotonously increases with increasing a/W.

Fig. 11 shows the results for $\beta = -0.2$. It is found that $F_I^{(b)}/F_{I\ homo}^{(b)}$ is in a small region 1.017–0.976, and it is seen that F_I is close to $F_{Imax}^{(b)}$, and F_{II} is close to $F_{IImax}^{(b)}$ individually. Fig. 12 shows the results for $\beta = -0.1$. Similarly to the case $\beta = -0.2$, it is found that $F_I^{(b)}/F_{I\ homo}^{(b)}$ is in the small region 1.004–0.909, and $F_I^{(b)}$ is close to $F_{Imax}^{(b)}$.
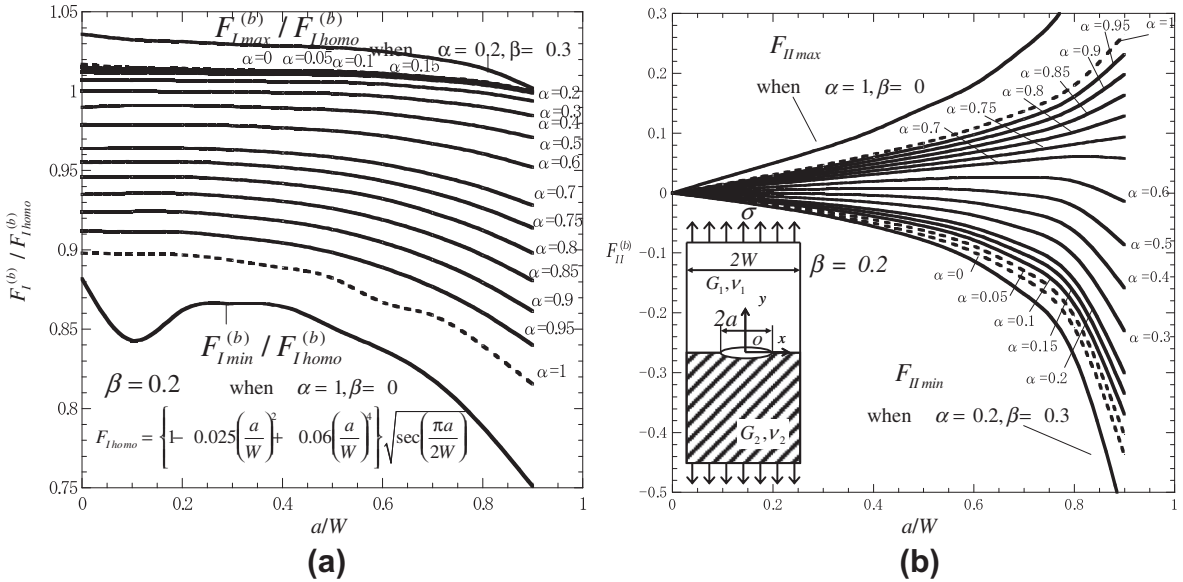

Fig. 15. (a) $F_I^{(b)}/F_{Ihomo}^{(b)}$ vs. a/W and (b) $F_{II}^{(b)}$ vs. a/W when $\beta = 0.2$.
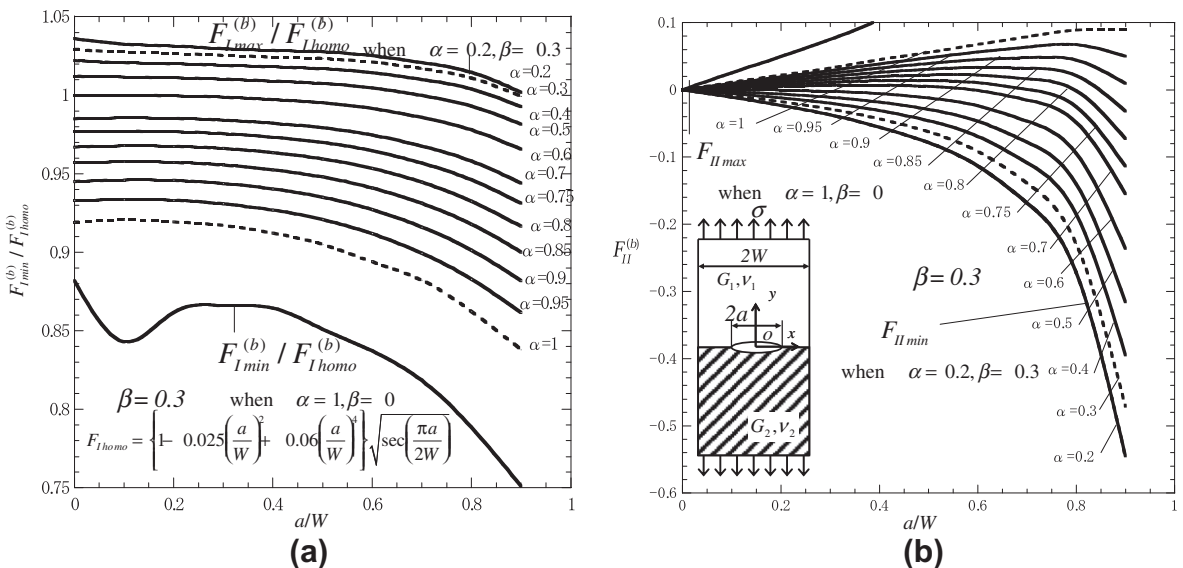

Fig. 16. (a) $F_I^{(b)}/F_{Ihomo}^{(b)}$ vs. a/W and (b) $F_{II}^{(b)}$ vs. a/W when $\beta = 0.3$.

On the other hand, when $\beta = 0$, the ratio $F_I^{(b)}/FIhomo^{(b)}$ largely depends on α and distributes in a wide region as 1.000–0.751. The ratio $F_I^{(b)}/F_{Ihomo}^{(b)}$ is close to 1 when α is small, and becomes smaller when α is large. When $\alpha = 1$, $F_I^{(b)}/F_{I\,homo}^{(b)}$ takes the minimum value for all regions of a/W. On the other hand, $F_{II}^{(b)}$ increases with increasing α, and the increment becomes larger when crack length is larger. For almost all regions of crack length, $F_{II}^{(b)}$ takes the maximum when $\alpha = 1$ except the case when crack length is extremely large.

Similar trend of Fig. 13 can be seen in Fig. 14 for $\beta = 0.1$ and in Fig. 15 for $\beta = 0.2$ although the distribution region is a little smaller in Figs. 14 and 15. On the other hand, $F_{II}^{(b)}$ is always positive when $\beta = 0$, but for $\beta = 0.1$ and $\beta = 0.2$ $F_{II}^{(b)}$ is positive value when α is large and negative when α is small.

For $\beta = 0.3$ in Fig. 16, it is seen that $F_I^{(b)}/F_{Ihomo}^{(b)}$ always takes the maximum value for a/W when $\alpha = 0.2$, and $F_{II}^{(b)}$ always takes the minimum value when $\alpha = 0.2$.
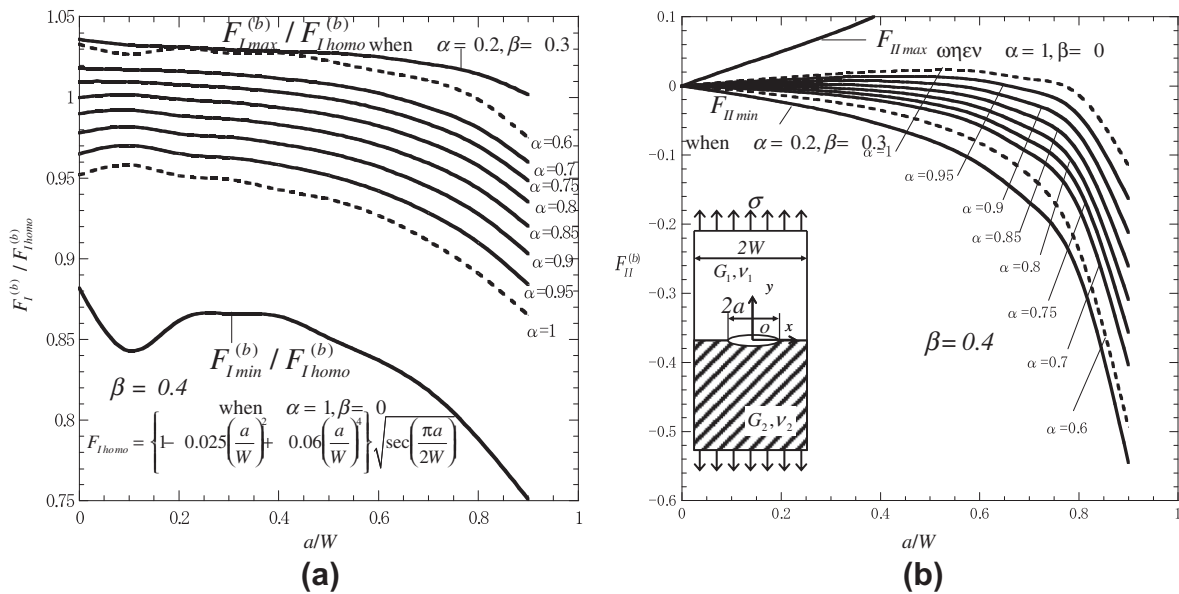

Fig. 17. (a) $F_I^{(b)}/F_{Ihomo}^{(b)}$ vs. a/W and (b) $F_{II}^{(b)}$ vs. a/W when $\beta = 0.4$.
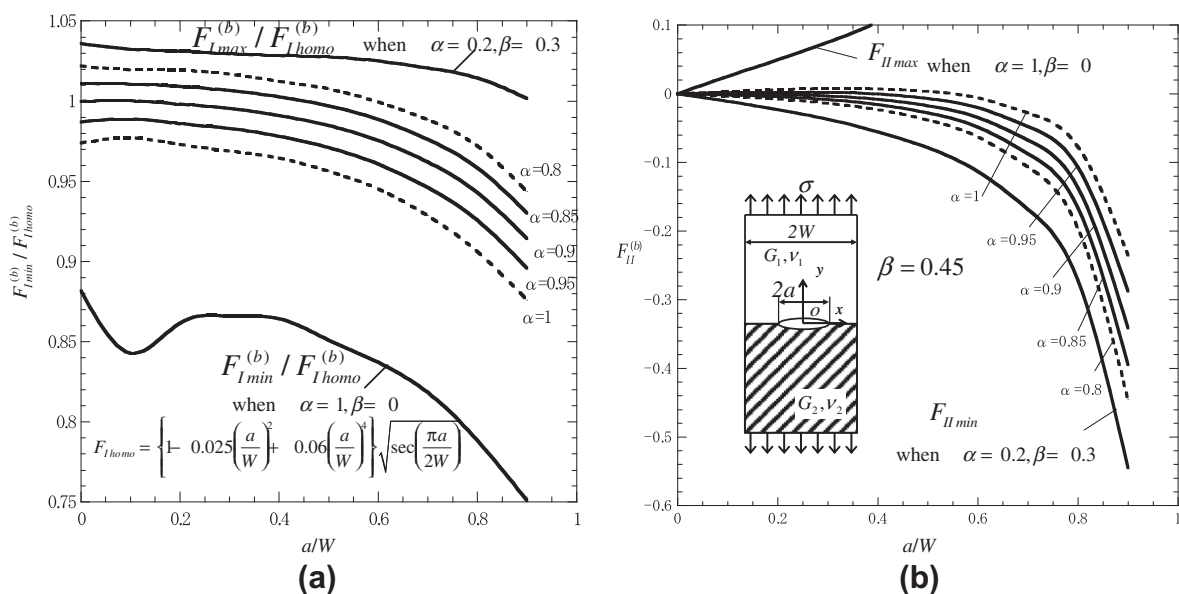

Fig. 18. (a) $F_I^{(b)}/F_{Ihomo}^{(b)}$ vs. a/W and (b) $F_{II}^{(b)}$ vs. a/W when $\beta = 0.45$.

Fig. 17 shows the case $\beta = 0.4$ and Fig. 18 shows the case $\beta = 0.45$. It is found that $F_I^{(b)}/F_{Ihomo}^{(b)}$ decreases with increasing crack length, and on the other hand, $F_{II}^{(b)}$ always has negative values for all a/W.

Considering $F_I^{(b)}/F_{Ihomo}^{(b)}$ when $a/W \leqslant 0.9$, it is known that $0.751 < F_I^{(b)}/F_{Ihomo}^{(b)} < 1.036$, and mostly it distributes in the region which is a little smaller than 1.

6. Comparison between periodic interface cracks and a center interface crack

In order to compare the results of Fig. 4a and b, the results of Fig. 4a are shown as $F_I^{(a)}/F_{Ihomo}^{(b)}$ in Fig. 19 when $\beta = 0$, and the results for the case when $\beta = 0.4$ are shown in Fig. 20. For periodic interface cracks, $F_I^{(a)}/F_{Ihomo}^{(b)}$ distributes within the region of $F_I^{(b)}/F_{Ihomo}^{(b)}$ except the case when the crack length is very large. For a fixed β, the results of periodic interface cracks are close to the results of a central interface crack in a bonded finite plate when α is small and the crack length is small. On the other hand, when, the results of periodic interface cracks are close to the results of a central interface crack in a bonded finite plate when α is large and the crack length is large.
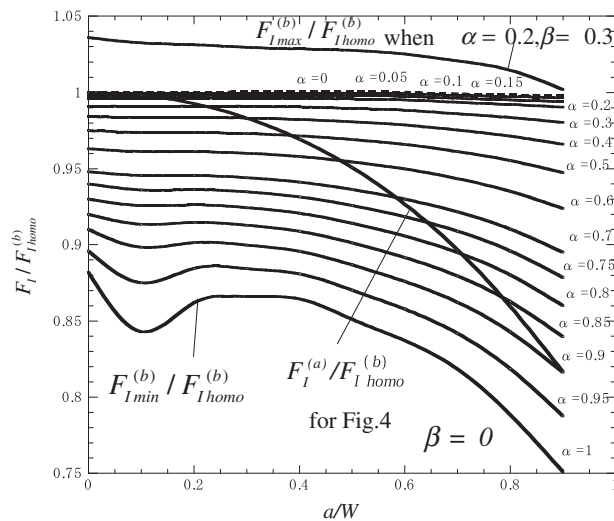

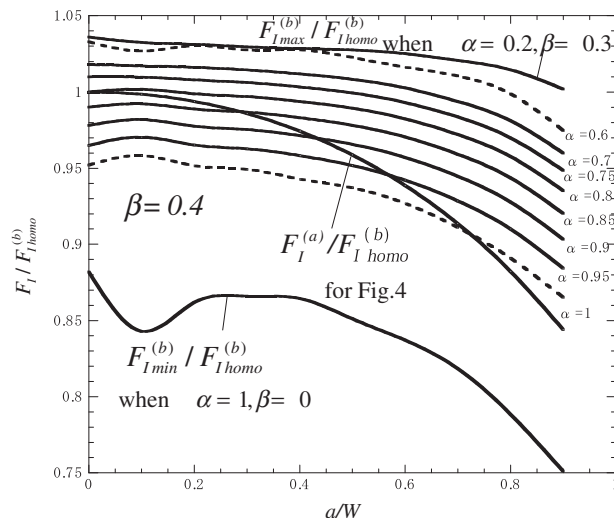**Fig. 19.** Comparison between the results in Fig. 4a and b when $\beta = 0$.

Fig. 20. Comparison between the results in Fig. 4a and b when $\beta = 0.4$.

7. Conclusion

In this paper, the stress values at the crack tip calculated by FEM are used and the stress intensity factors of interface cracks are evaluated from the ratio of stress values between a reference problem and a given problem. Then the stress intensity factors are discussed with the following conclusions.

(1) For periodic interface cracks in a bonded plate shown in Fig. 4a, the effects of relative crack length and material combinations on the stress intensity factors have been discussed. Stress intensity factors $F_I^{(a)}$, $F_{II}^{(a)}$ increase with increasing ε (Fig. 9 and Table 5).

(2) For a central interface crack in a bonded finite plate shown in Fig. 4b, the effects of relative crack length and material combinations on the stress intensity factors have been discussed. The ratio to the results to the homogeneous material $F_I^{(b)}/F_{Ihomo}^{(b)}$ is in the region $0.751 < F_I^{(b)}/F_{Ihomo}^{(b)} < 1.036$ when $a/W \leqslant 0.9$, and mostly it distributes in the region which is a little smaller than 1.

Generally, F_I always takes the maximum value when $\alpha = 0.2$, $\beta = 0.3$ and minimum value when $\alpha = 1.0$, $\beta = 0$. On the other hand, F_{II} always takes the maximum value when $\alpha = 1.0$, $\beta = 0$ and minimum value when $\alpha = 0.2$, $\beta = 0.3$ except the case when the crack length is extremely large.

(3) From the comparison between the results for periodic interface cracks and a central interface crack in a finite bonded plate, it is seen that the results of periodic interface cracks are close to the results of a central interface crack in a bonded finite plate when α is small and the crack length is small. The results of periodic interface cracks are close to the results of a central interface crack in a bonded finite plate when α is large and the crack length is large.

References

[1] Yuki Y. Mech Interface, Baifuukan 1992 (in Japanese).
[2] Nao-Aki Noda, Yu Zhang, Xin Lan, Yasushi Takase, Kazuhiro Oda. Stress intensity factor of an interface crack in a bonded plate under uni-axial tension. J Solid Mech Mater Eng 2009;4(7):974–87.
[3] Oda K, Kamisugi K, Noda NA. Stress intensity factor analysis of interface cracks based on proportional method. Trans Jpn Soc Mech Eng 2009;A-75:467–82 (in Japanese).
[4] Teranisi T, Nisitani H. Determination of highly accurate values of stress intensity factor in a plate of arbitrary form by FEM. Trans Jpn Soc Mech Eng 1999;A-65:16–21 (in Japanese).
[5] Nisitani H, Teranisi T, Fukuyama K. Stress intensity factor analysis of a biomaterial plate based on the crack tip stress method. Trans Jpn Soc Mech Eng 2003;A-69:1203–8 (in Japanese).
[6] Westergaard HM. Bearing pressures and cracks. J Appl Mech 1939;61:49–53.
[7] Irwin GR. Fracture. Handbuch der Physik 1958;VI:551–90.
[8] Koiter W T. An infinite row of collinear cracks in an infinite elastic sheet. Ing Arch 1959;28:168–72.
[9] Isida M. Elasticity analysis and stress intensity factor of crack. Baifuukan 1976 (in Japanese).
[10] Okamura H. Introduction linear fracture mechanics. Baifuukan 1990 (in Japanese).